PNAS
www.pnas.org

Supplementary Information for

Basal forebrain mediates prosocial behavior via disinhibition of midbrain dopamine neurons

Jun Wang[1], Jie Li[1], Qian Yang[1], Ya-Kai Xie, Ya-Lan Wen, Zhen-Zhong Xu, Yulong Li, Tianle Xu, Zhi-Ying Wu, Shumin Duan, and Han Xu*

[1]These authors contributed equally to this work.

*Corresponding author:

Han Xu, Ph.D., Professor

School of Brain Science and Brain Medicine

Zhejiang University School of Medicine

Hangzhou, Zhejiang 310058, China

Phone: +86-571-88208978

Email: xuhan2014@zju.edu.cn

This PDF file includes:

Materials and Methods

Animals.

Adult SST-Cre (JAX Strain 013044), vGluT2-Cre (JAX Strain 016963), vGAT-Cre (JAX Strain 016962) and C57BL/6J wild-type male mice (2-4 months old) were used in this study. All animals were group housed in a 12 h light/dark cycle with food and water *ad libitum* except for food preference test in which mice were fasted overnight. Behavioral experiments were conducted during the animals' light cycle. Before behavioral tests, animals were habituated to the experimenter by handling for at least 3 consecutive days (15 min per day). Animal care and use were under the guidelines approved by the Animal Care and Use Committee of Zhejiang University.

Virus Preparation.

AAV2/9-EF1α-double floxed-hChR2(H134R)-mCherry (3.40×10^{12} genomic copies per ml), AAV2/9-EF1α-DIO-eNpHR3.0-EYFP (2.50×10^{12} genomic copies per ml), AAV2/9-EF1α-DIO-eNpHR3.0-mCherry (2.70×10^{12} genomic copies per ml), AAV2/9-hSyn-DIO-GCaMP6m (2.90×10^{12} genomic copies per ml), AAV2/9-hSyn-$GRAB_{DA2m}$ (3.76×10^{13} genomic copies per ml), AAV2/9-hSyn-FLEX-ChrimsonR-tdTomato (3.72×10^{12} genomic copies per ml), AAV2/9-EF1α-DIO-EYFP (3.25×10^{12} genomic copies per ml), AAV2/9-EF1α-DIO-mCherry (3.08×10^{12} genomic copies per ml), and AAV2/9-hSyn-FLEX-mGFP-Synaptophysin-mRuby (4.80×10^{12} genomic copies per ml) were purchased from Taitool (Shanghai), Obio Technology (Shanghai), BrainVTA (Wuhan) or Vigene Biosciences (Jinan). The virus solutions were aliquoted over ice into 0.2 ml vials and stored immediately in freezer after arrival. The stock solutions were thawed to room temperature and vortexed for a few seconds before use.

Virus Injection.

Mice were anesthetized with isoflurane (4% for induction, 1% for maintenance) and placed in a stereotaxic frame (Stoelting Co., IL, USA). The skull was exposed under a surgical microscope and a small craniotomy was

made with a dental drill. The following coordinates relative to bregma were used to target the caudal portion of the BF (including the horizontal limb of the diagonal band of Broca, magnocellular preoptic nucleus and substantia innominata) (AP, +0.15 mm; ML, ±1.40 mm; DV, -5.70 mm), NAc (AP, +1.25 mm; ML, ±0.75 mm; DV, -4.20 mm), MPO (AP, 0.00 mm; ML, ±0.40 mm; DV, -5.10 mm). A small volume of virus solution (100 to 300 nL) was injected into the target regions at a slow rate (20 to 40 nL/min) using a glass micropipette (tip diameter ~20 μm) attached to a Nanoliter pressure microsyringe pump and a micro controller (World Precision Instrument). Virus was injected bilaterally for optogenetic manipulation, and unilaterally for fiber photometry or viral tracing. To allow virus diffusion, the injection pipette was remained in place for another 10 min at the end of the infusion. Experiments were conducted at least 2 weeks, 4 weeks, 6 weeks and 8 weeks after virus injection for fiber photometry, cell bodies stimulation, axon terminals stimulation and neural tracing, respectively.

Optical Fiber Implantation.

For optogenetic manipulation and fiber photometry experiments, the optical fiber implantation was carried out at least 2 weeks ahead of behavioral testing. An optical fiber (OD: 200 μm, NA: 0.37; Inper Inc.) was placed in a ceramic ferrule (OD: 1.25 mm) and inserted toward the targeted brain regions (with the tip 200 μm above) through the craniotomy. For optogenetic manipulation, two optical fibers were implanted to target bilateral BF, VTA or LHb using the following coordinates: BF (AP, +0.15 mm; ML, ±1.40 mm; DV, -5.50 mm), VTA (AP, -2.80 mm; ML, ±1.54 mm at a 10° angle; DV, -4.36 mm), LHb (AP, -1.70 mm; ML, ±0.88 mm at a 10° angle; DV, -2.43 mm). For fiber photometry, one optical fiber was implanted to target unilateral BF or NAc using the following coordinates: BF (AP, +0.15 mm; ML, ±1.40 mm; DV, -5.50 mm), NAc (AP, +1.25 mm; ML, ±0.75 mm; DV, -4.00 mm). The ceramic ferrule was secured to the skull using 3M Vetbond tissue adhesive and dental cement.

Fiber Photometry.

Fiber photometry system (ThinkerTech, Nanjing) was used to record fluorescence signals emitted by GCaMP6m (a genetically encoded calcium indicator) or $GRAB_{DA2m}$ (an optimized genetically encoded DA sensor). During recordings, a laser beam (473 nm) was reflected by a dichroic mirror (MD498; Thorlabs) and then coupled to an optical commutator (Doric Lenses). An optical fiber guided the light between the commutator and the implanted optical fiber. The laser power was adjusted at the tip of optical fiber to a low level (20-40 μW) to minimize bleaching and kept constant during a recording session. The fluorescence signals were bandpass filtered and collected by a photomultiplier tube (R3896, Hamamatsu). The photomultiplier tube current output was converted to voltage signals, which was further filtered through a low-pass filter (40 Hz cut-off; Brownlee 440). The analog voltage signals were digitalized at 100 Hz and recorded using a custom-written script in LabView. Animal behavior was simultaneously recorded with the EthoVision XT video tracking system (Noldus, Netherland). Behavior-coupled fluorescence transients were determined by peri-stimulus time histograms (PSTH) calculated as ΔF/F.

Detection of DA Efflux in the NAc.

To examine the role of BF SST→VTA or MPO→VTA projections on NAc DA efflux during social interaction, BF SST or MPO GABA neurons were virally infected with NpHR opsins. Four weeks later, $GRAB_{DA2m}$ was virally expressed in the NAc and an optical fiber was implanted unilaterally in the NAc and two optical fibers were implanted bilaterally in the VTA. Animals were allowed to recover for two weeks and the $GRAB_{DA2m}$ fluorescence signals were then monitored with fiber photometry throughout behavioral test. Constant photostimuli (589 nm, 5-8 mW) were delivered to the VTA alternatively among trials when test mice interacting with a juvenile mouse in an open field arena. The difference in fluorescence signal changes between Light off trials and Light on trials of individual test mice reflect the effect of BF SST→VTA or MPO→VTA projections on NAc DA efflux during social interaction. To test whether activation of BF SST→VTA projections can trigger DA release in the NAc, BF SST neurons were virally infected with ChrimsonR opsins. The $GRAB_{DA2m}$ fluorescence signals were

monitored with fiber photometry in an open field arena. Five millisecond yellow light pulses (589 nm, 5-8 mW) was delivered to the VTA at 30 Hz for 1 s with a 10 s inter-trial interval. Light-coupled fluorescence transients were determined by peri-stimulus time histograms (PSTH) calculated as ΔF/F.

Optogenetic Stimulation during Behavior.

For optogenetic inhibition experiments, two optical fibers were bilaterally implanted in the BF, VTA or LHb right after NpHR virus injection. With an optical fiber sleeve, an optical fiber (200 μm in diameter) was connected to a laser generator (Inper INc., Hangzhou). The laser beam (589 nm) was split into two beams through a commutator and connected to the implanted optical fibers. The animals were then placed in the three-chamber, two-chamber or open field testing apparatus. The power of photostimulation was 5-8 mW measured at the tip of the optical fiber and was constantly delivered as required. Control mice injected with EYFP virus underwent the same procedure and received the same amount of photostimulation.

Three-Chamber Social Interaction Test.

Animals were allowed to acclimate to the behavioral testing room for at least 1 h before the first trial began. The apparatus consisted of a three-compartment white Plexiglas box. Two identical cylinder-shaped acrylic cages (10 cm in diameter) were placed in the middle of each side compartment during testing session. A test mouse was placed in the middle compartment and was allowed to freely explore the apparatus for 10 min. After this habituation period, a male juvenile mouse (3-5 weeks old) was placed inside the cylinder cage in one of the side compartments designated as the social chamber and a toy mouse in the other cylinder cage of the opposite compartment designated as the neutral chamber. The lower 10 cm wall of the acrylic cages had evenly distributed slots (1 cm width) to allow the test mouse to interact with the juvenile mouse or the toy mouse. Social chamber was randomly chosen and counterbalanced for each group. The test mouse was allowed to freely explore all three compartments of the apparatus for another 10 min. The overall activity of the test mouse in the

apparatus was automatically recorded with the EthoVision XT video tracking system (Noldus, Netherland). The amount of time that test mice spent in each chamber or in the immediate vicinity (5 cm) of the cages (termed as “zone”) was measured. The social interaction index is calculated as the difference in the time spent in the social and neutral chambers (zones), divided by the sum of the time spend in both chambers (zones). After each session, the apparatus and cylinder cages were thoroughly cleaned with 75% ethanol to prevent olfactory cue bias.

Three-Chamber Food Preference Test.

Mice were fasted 12 h before behavioral test. A test mouse was placed in the middle compartment and was allowed to freely explore the apparatus for 10 min. After this habituation period, standard food chows were placed inside the cylinder cage in one of the side compartments designated as the chow chamber and amount- and appearance-matched objects in the other cylinder cage of the opposite compartment designated as the object chamber. The test mouse was allowed to freely explore all three compartments of the apparatus for another 10 min. The overall activity of the test mouse in the apparatus was automatically recorded with the EthoVision XT video tracking system (Noldus, Netherland). The amount of time that test mice spent in each chamber or in the immediate vicinity (5 cm) of the cages (termed as “zone”) was measured. The food preference index calculated as the difference in the time spent in the food and object chambers (zones), divided by the sum of the time spent in both chambers (zones). After each session, the apparatus and cylinder cages were thoroughly cleaned with 75% ethanol to prevent olfactory cue bias.

Real-Time Place Avoidance (RTPA) Test.

The testing apparatus was a clear Plexiglas box (40 × 40 × 20 cm) that was divided into 2 equal compartments by a plastic divider with a 10 cm wide rectangular opening in the middle. Test mice implanted with optical fibers were connected to a laser generator through a commutator. The mice were then allowed to habituate to the apparatus for 15 min. Those mice with no bias to either compartment were further used for a 15 min RTPA assay, during which

mice were allowed to freely explore both compartments. Constant photostimuli (589 nm; 5-8 mW) were delivered each time when the test mice entered one randomly selected compartment. The overall activities of the mice were automatically recorded using the Ethovision XT video tracking system (Noldus, Netherland). The percentage of time spent in the stimulated chamber was calculated to evaluate their avoidance tendency. The testing apparatus was thoroughly cleaned with 75% ethanol between tests.

Open Field Test.

The open field test was conducted in an open field arena (50 × 50 × 50 cm) to evaluate animals' locomotor activity and anxiety-like behavior. Mice were allowed to freely explore the arena for 10 min while constant photostimuli were delivered through the implanted optical fibers. The animals' movement was automatically monitored using the Ethovision XT video tracking system (Noldus, Netherland). The total distance traveled, time spent in the center zone (25 cm square) and the number of center entries were analyzed. The arena was thoroughly cleaned with 75% ethanol between tests.

Brain Slice Preparation.

SST-Cre mice expressed AAV-DIO-ChR2-mCherry or AAV-DIO-eNpHR3.0-EYFP in the BF for at least 6 weeks were used for brain slice preparation. Briefly, mice were deeply anesthetized with pentobarbital sodium (i.p., 100 mg/kg body weight) and transcardially perfused with 20 ml ice-cold oxygenated modified ACSF containing (in mM) 87 NaCl, 2.5 KCl, 1.25 NaH_2PO_4, 26 $NaHCO_3$, 1 $CaCl_2 \cdot 2H_2O$, 2 $MgSO_4 \cdot 7H_2O$, 75 sucrose and 10 glucose. The brain was then quickly dissected and coronal slices (250 μm) containing the BF, VTA or LHb were generated using a microtome (Leica VT1200s, Germany). The brain slices were incubated in a holding chamber at 32 °C for 30 min followed by continued incubation at room temperature for at least 1 h with standard ACSF containing (in mM) 119 NaCl, 2.5 KCl, 1.25 NaH_2PO_4, 24 $NaHCO_3$, 2 $CaCl_2 \cdot 2H_2O$, 2 $MgSO_4 \cdot 7H_2O$, and 12.5 glucose (pH: 7.4 when bubbled with 95% O_2 and 5%

CO_2; osmolarity: 300-305 mOsm/kg). All chemicals used in slice preparation were purchased from Sigma.

Whole-Cell Patch Clamp Recordings.

A brain slice was transferred to a recording chamber (Warner Instruments Inc., Hamden, CT) that was maintained at 30-32°C with a heater controller (TC-324B, Warner Instruments), and was continuously perfused with fully oxygenated standard ACSF at a rate of 2 ml/min. Whole-cell patch-clamp recordings were obtained from visually identified neurons using a 40× water-immersion objective on an upright microscope (Olympus, Japan) equipped with IR-DIC optics and a CCD camera. Patch electrodes (5-8 MΩ) were pulled from borosilicate glass capillaries (1.5 mm OD) with a P-97 puller (Sutter Instrument, Novata, CA), and filled with internal solution containing (in mM) 65 K-gluconate, 65 KCl, 0.5 EGTA, 10 HEPES, 4 Mg-ATP, 0.3 Na-GTP and 5 phosphocreatine (pH, 7.2-7.3; osmolarity, 285-290 mOsm/kg). Data were collected using a Multiclamp 700B amplifier (Molecular Devices, Sunnyvale, CA), low-pass filtered at 5 kHz and digitally samples at 10 kHz on-line and analyzed off-line with pClamp9 software (Molecular Devices). Series resistances were compensated by ~70% and only cells with stable series resistance (<20% change over the recording period) were used for analysis. To measure the hyperpolarization-activated current (I_h), neurons were held at -70 mV in voltage-clamp mode and stepped to more negative potentials in 5 mV increments.

Optogenetic Stimulation in Slices.

Photostimuli were produced by LEDs (Mightex, Toronto, Canada) and delivered through a 40X water immersion objective. To examine the efficiency of NpHR in hyperpolarizing BF SST neurons, the neurons were recorded in a current-clamp mode with 0 pA or 180 pA current injection and a yellow light stimulation (589 nm, 5-10 mW, 250 ms) was delivered every 5 s. To record synaptic currents in VTA neurons, the neurons were held at -70 mV in voltage-clamp mode and a blue light pulse (470 nm, 5-10 mW, pulse width 2 ms) was delivered every 10 s to stimulate the ChR2-expressing axon terminals of BF SST

neurons. To confirm the inhibitory nature of the light evoked postsynaptic currents, 10 μM bicuculline was added to the bath solution to block the $GABA_A$ receptors. The amplitude of I_h current was defined as the difference between the instantaneous current at the beginning of a hyperpolarizing voltage step (-120 mV, 500 ms) and the instantaneous current at the end of the voltage step. To verify the function of NpHR-terminal suppression, sIPSCs were recorded at -70 mV with bath application of 6,7-dinitroquinoxaline- 2,3-dione (DNQX, 10 μM) and DL-2-Amino-5-phosphonopentanoic acid (AP-5, 20 μM).

Anterograde Tracing.

Synaptic tracer AAV2/9-hSyn-FLEX-mGFP-Synaptophysin-mRuby was used to trace the output targets of BF SST neurons. At least 8 weeks after virus injection, mice were euthanized and perfused. Then 40 μm frozen brain sections were collected. Fluorescent images of LHb and VTA were captured using a confocal microscope (Olympus FV1200) with a 10X objective and boundaries were defined based on DAPI staining. To visualize the projecting pattern across the rostral-caudal extent of the VTA, two sections per atlas image were selected and ImageJ software was used for analysis. The integrated pixel densities were measured for each VTA subregion and were normalized to the total pixel density of all subregions for individual animals.

Immunohistochemistry.

Mice were deeply anesthetized and subsequently transcardially perfused with 20 ml PBS followed by 30 ml cold 4% PFA (pH 7.4). Brains were extracted and post-fixed in 4% PFA solution overnight and then transferred to a 30% sucrose solution at 4 °C until the brains sank. Brains were coronally sectioned into 40 μm slices in a cryostat (Leica CM1950). For checking virus expressing, sections were washed twice with PBS and incubated in a DAPI solution (1:50,000) for 5 min, washed three times with PBS and the mounted onto slides for microscope imaging. For immunohistochemistry experiments, sections were washed twice with PBS and then incubated in blocking solution (10% normal goat serum, 1% BSA, and 0.3% Triton X-100 in PBS) for 1 h at room temperature. Sections were

then incubated in primary antibody solution overnight at 4 °C. The following primary antibodies were used: rabbit anti-somatostatin (1:1000; Cat# T-4103, Peninsula Laboratories LLC), rabbit anti-GFP (1:1000, Cat# ab6556, Abcam). After three times washed, the brain slices were incubated in Alexa Fluor 594-conjugated goat anti-rabbit (1:1000, Cat# ab150080, Abcam) or Alexa Fluor 488-conjugated goat anti-rabbit (1:1000, Cat# ab150077, Abcam) secondary antibody for 1.5 h at room temperature. The brain slices were finally washed and mounted onto glass slides.

To determine the cell-type identity of recorded neurons, neurobiotin (0.1%) was added into the internal solution in patch clamp recordings, and brain slices were subsequently processed with immunohistochemistry. The brain slices were fixed in 4% paraformaldehyde (PFA) overnight at 4 °C, then washed three times with phosphate-buffered saline (PBS), followed by blocked in PBS containing 0.3% Triton X-100 and 10% normal goat serum for 1.5 h at room temperature. Then the brain slices were incubated in rabbit anti-TH (1:1000, Cat# AB152, Millipore) or rabbit anti-GABA (1:500, Cat# A2052, Sigma) for 24 h at 4 °C. After three times washed with PBS, the brain slices were incubated in Alexa Fluor 594-conjugated goat anti-rabbit secondary antibody (1:1000, Cat# ab150080, Abcam) for 1.5 h at room temperature. The brain slices were finally washed and mounted onto glass slides for microscope imaging.

Fluorescent images were captured using a confocal microscope (Olympus FV1200) with a 10X or 20X objective to verify virus expression and for cell counting. Scans from each channel were collected in multi-track mode to avoid cross-talk between channels.

RNAscope in situ Hybridization.

RNAscope multiplex fluorescent reagent kit v2 (323100, ACDbio) and immunolabeling was used on brain slices expressing DIO-GCaMP6m to verify the virus expression in vGluT2 neurons. Mice were deeply anesthetized and transcardially perfused with RNA-free PBS and cold 4% PFA (pH 7.4). Brains were post-fixed in 4% PFA solution overnight and then immersed in 30% sucrose solution made with RNA-free PBS. Coronal brain slices (20 μm) of the BF were

sectioned and were mounted onto slides. The RNAscope assay was performed according to the manufacturer's standard protocols. Sections were treated with protease digestion and heat followed by hybridization which contains target probes to mouse vGluT2 (319171, ACDbio). After completion of RNAscope for vGluT2, immunostaining for EGFP was conducted to amplify fluorescence signals of GCaMP6m.

Statistics.

Data are presented as mean ± SEM unless otherwise noted. Statistical comparisons were conducted with GraphPad Prism 7 (La Jolla, CA) for all behavioral and electrophysiological experiments and with MATLAB for fiber photometry experiments. Generally, one-way or two-way ANOVA followed by Bonferroni *post hoc* test was performed for multiple comparisons, unpaired *t* test or Mann-Whitney *U* test was performed for two-group comparisons, and Fisher's exact test was performed for analysis of contingency tables as specified in figure legends. A p value of < 0.05 was considered as statistically significant. $*P < 0.05$, $**P < 0.01$, $***P < 0.001$, $****P < 0.0001$.

Supplementary Figures

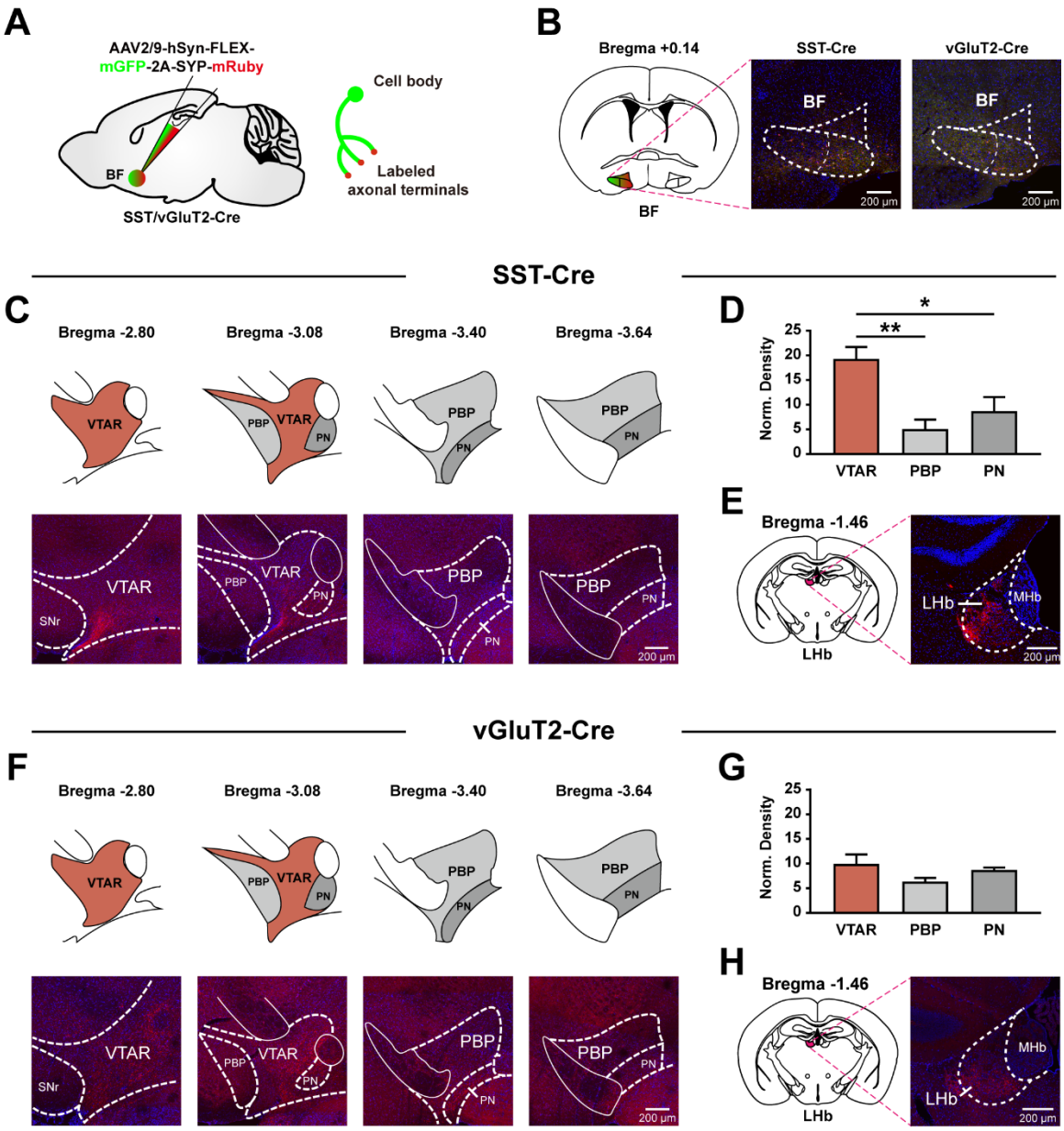

Fig. S1. Anterograde tracing of BF SST and vGluT2 neuron projections to the VTA and LHb.

(*A*) Schematic illustration of AAV2/9-hSyn-FLEX–mGFP-2A-SYP-mRuby injection in the BF of SST-Cre or vGluT2-Cre mice.

(*B*) Coronal schematic showing viral injection site (Left) and representative confocal images showing targeted AAV2/9-hSyn-FLEX–mGFP-2A-SYP-mRuby expression in the BF of SST-Cre (Middle) and vGluT2-Cre mice (Right).

(*C*) Top: coronal schematic showing the VTAR, PBP and PN subdivisions of the VTA along the rostral-caudal axis. Bottom: representative confocal images showing the distribution of SYP:mRuby puncta in three subdivisions of the VTA of SST-Cre mice. VTAR: rostral VTA; PBP: parabrachial pigmented region; PN: the paranigral region.
(*D*) Quantification of integrated pixel densities of SYP:mRuby puncta in subdivisions of the VTA. Error bars indicate mean ± SEM (*n* =15 slices from 3 mice). *$P < 0.05$; **$P < 0.01$; one-way ANOVA followed by Bonferroni *post hoc* analysis.
(*E*) Coronal schematic showing the site of LHb (Left) and the representative confocal image (Right) showing the distribution of SYP:mRuby puncta in the LHb of SST-Cre mice.
(*F*-*H*) The same as (*C*-*E*) but for vGluT2-Cre mice. Error bars indicate mean ± SEM (*n* =10 slices from 2 mice).

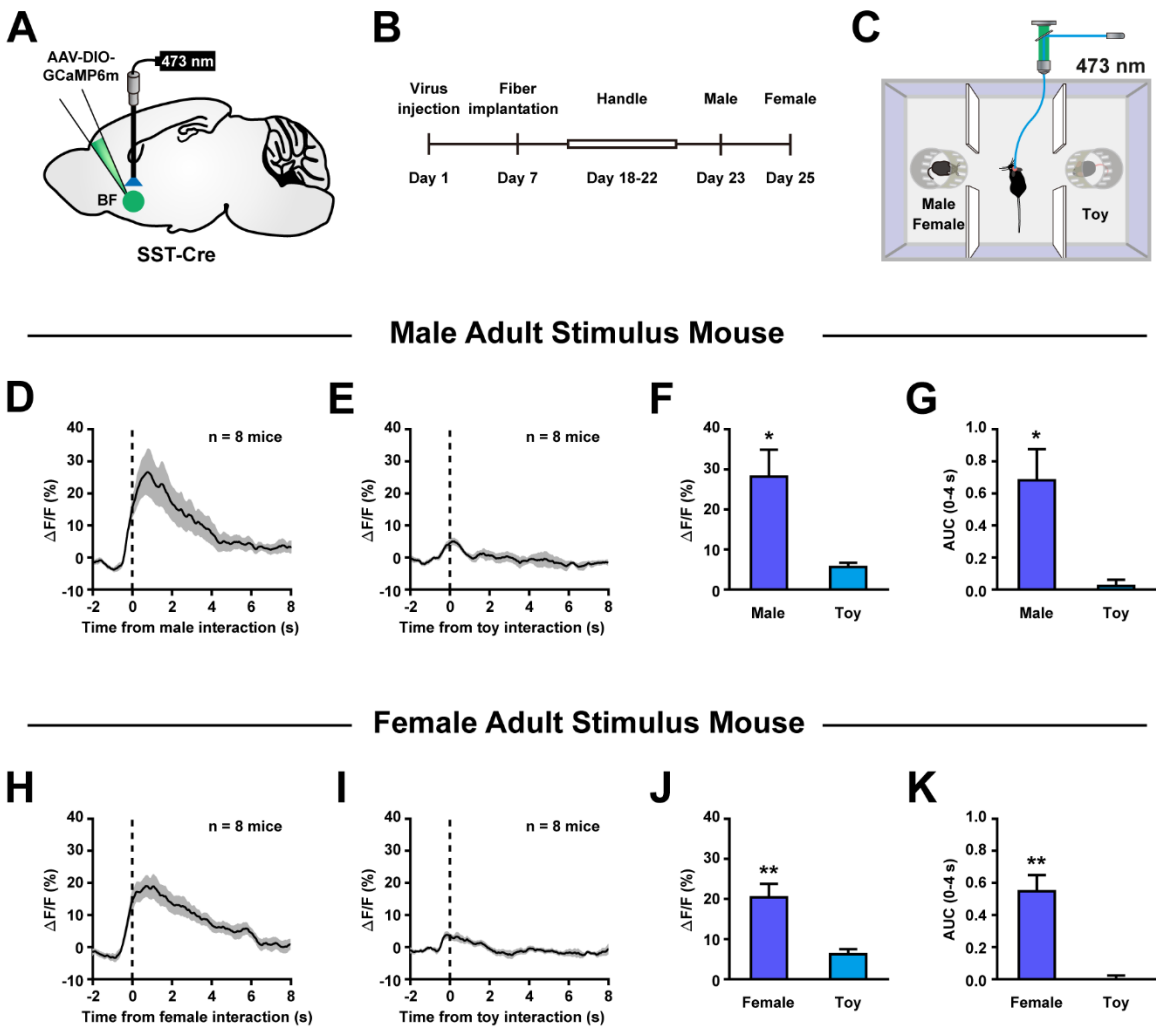

Fig. S2. BF SST neurons are activated during social interaction with male or female adult stimulus mouse.

(*A*) Schematic diagram of virus injection and optical fiber implantation.

(*B*) Time course of the experimental design. Day 1: Unilateral injection of AAV-DIO-GCaMP6m in the BF of SST-Cre mice. Day 7: Fiber implantation over the BF for photometric recording. Day 18-22: Gently handling by the experimenter. Day 23: Photometric recording during social interaction with a male adult mouse. Day 25: Photometric recording during social interaction with a female adult mouse.

(*C*) Schematic illustration of photometric recording.

(*D*) The peri-event plot of the mean Ca^{2+} transient during male adult stimulus mouse interaction for the entire test group (*n* = 8 mice). The thick line indicates mean and the shaded area indicates SEM.
(*E*) The same as (*D*) but for toy mouse interaction.
(*F-G*) Statistic comparison of fluorescence signals of BF SST neurons between male adult mouse interaction and toy mouse interaction. Error bars indicate mean ± SEM. **P* < 0.05, paired t test.
(*H-K*) The same as (*D-G*) but for the female adult stimulus mouse interaction. Error bars indicate mean ± SEM. ***P* < 0.01; paired *t* test.

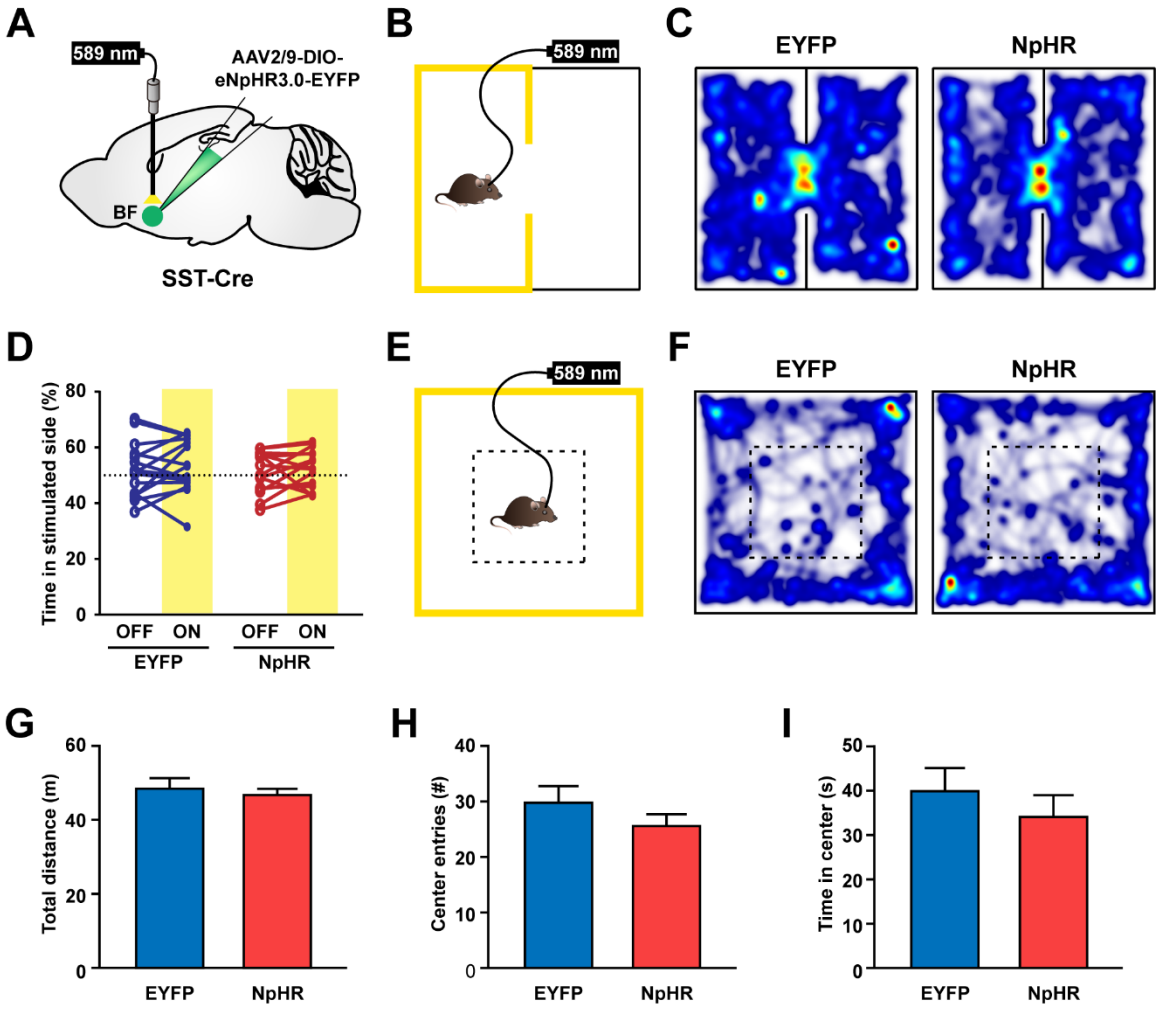

Fig. S3. Optogenetic inhibition of BF SST neurons does not produce RTPA and does not alter locomotion or general anxiety.

(*A*) Schematic illustration of eNpHR3.0-EYFP virus injection and optical fiber implantation in the BF.

(*B*) Schematic diagram showing the behavioral paradigm of a two-chambered RTPA test, where one chamber was paired with constant yellow light stimulation (589 nm, 5-8 mW).

(*C*) Representative heatmaps showing the locations of an EYFP-expressing control mouse (Left) and an NpHR-expressing experimental mouse (Right) in the RTPA test.

(*D*) Quantification of relative time spent in the stimulated chamber and non-stimulated chamber of EYFP and NpHR mice.

(*E*) Schematic diagram showing the behavioral paradigm of an open field test, where constant yellow light (589 nm, 5-8 mW) was delivered throughout the 10 min test for either EYFP or NpHR mice.
(*F*) Representative heatmaps showing the locations of an EYFP-expressing control mouse (Left) and an NpHR-expressing experimental mouse (Right) in an open field test.
(*G*-*I*) Quantification of total distance moved (*G*), number of center entries (*H*) and time in center (*I*) by EYFP and NpHR mice in an open field test.
Error bars indicate mean ± SEM (EYFP mice, $n = 15$; NpHR mice, $n = 15$).

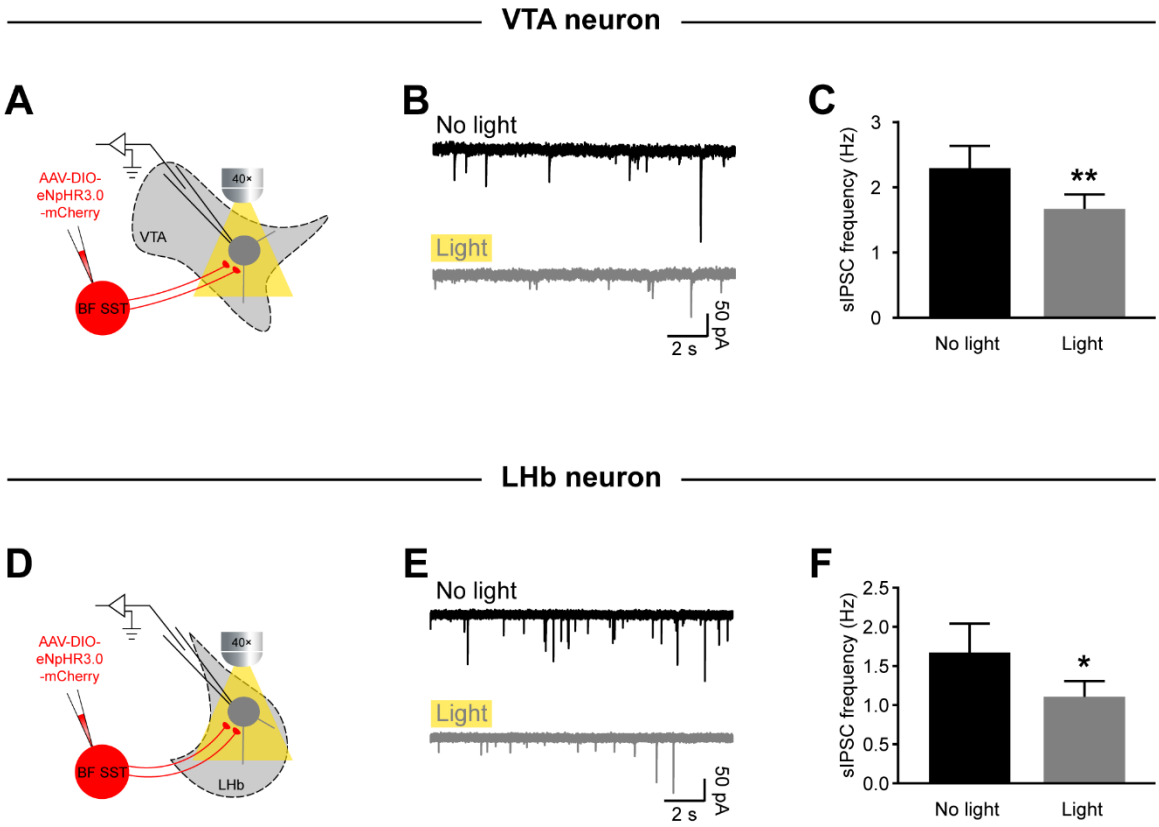

Fig. S4. Optogenetic inhibition of BF SST terminals in the VTA and LHb suppresses GABA release.

(*A*) Schematic illustration of eNpHR3.0-mCherry virus injection in the BF and patch-clamp recording in acute VTA slices.

(*B*) Example traces of spontaneous inhibitory postsynaptic currents (sIPSCs) recorded from VTA GABA neurons before and during constant yellow light stimulation.

(*C*) Quantification revealed that yellow light suppressed sIPSCs frequency in VTA GABA neurons (*n* = 21 neurons from 10 mice). Error bars indicate mean ± SEM. **P < 0.01; paired t test.

(*D-F*) The same as (*A-C*) but for LHb neurons (*n* = 11 neurons from 5 mice). Error bars indicate mean ± SEM. *P < 0.05; paired t test.

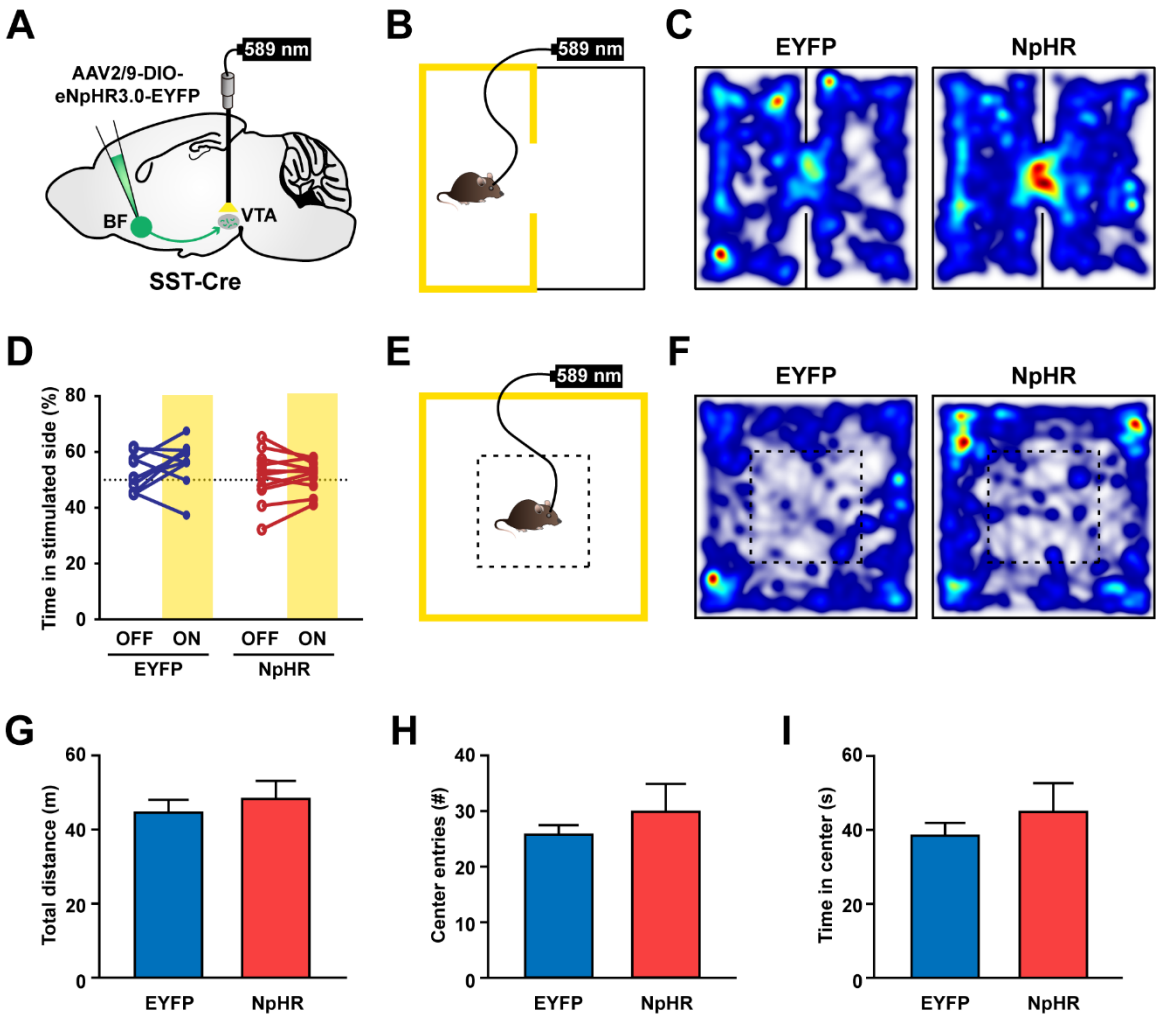

Fig. S5. Optogenetic inhibition of BF SST→VTA projections does not produce RTPA and does not alter locomotion or general anxiety.

(*A*) Schematic illustration of eNpHR3.0-EYFP virus injection in the BF and optical fiber implantation in the VTA.

(*B*) Schematic diagram showing the behavioral paradigm of a two-chambered RTPA test, where one chamber was paired with constant yellow light stimulation (589 nm, 5-8 mW).

(*C*) Representative heatmaps showing the locations of an EYFP-expressing control mouse (Left) and an NpHR-expressing experimental mouse (Right) in the RTPA test.

(*D*) Quantification of relative time spent in the stimulated chamber and non-stimulated chamber of EYFP and NpHR mice.

(*E*) Schematic diagram showing the behavioral paradigm of an open field test, where constant yellow light (589 nm, 5-8 mW) was delivered throughout the 10 min test for either EYFP or NpHR mice.
(*F*) Representative heatmaps showing the locations of an EYFP-expressing control mouse (Left) and an NpHR-expressing experimental mouse (Right) in an open field test.
(*G*-*I*) Quantification of total distance moved (*G*), number of center entries (*H*) and time in center (*I*) by EYFP and NpHR mice in an open field test.
Error bars indicate mean ± SEM (EYFP mice, $n = 10$; NpHR mice, $n = 11$).

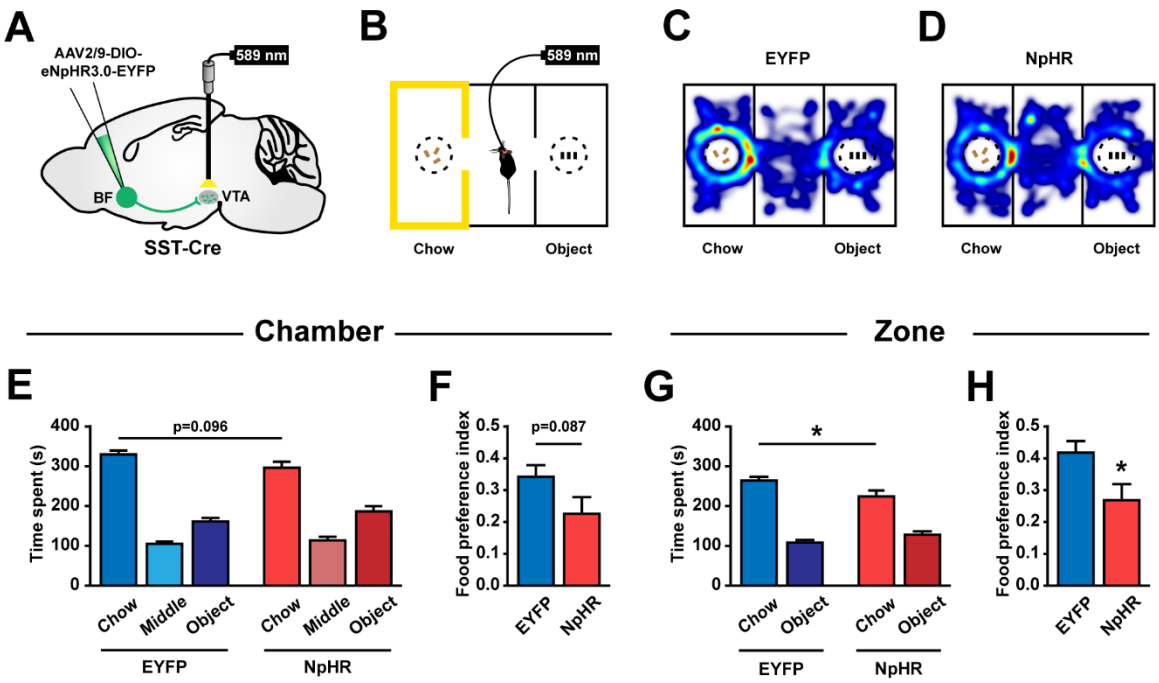

Fig. S6. Optogenetic inhibition of BF SST→VTA pathway reduces food preference.

(*A*) Schematic illustration of eNpHR3.0-EYFP virus injection in the BF and optical fiber implantation in the VTA.

(*B*) Schematic illustration of an experimental mouse subjected to a three-chamber food preference test, where the chow chamber was paired with constant yellow light stimulation (589 nm, 5-8 mW).

(*C* and *D*) Representative heatmaps showing the locations of an EYFP-expressing control mouse (*C*) and an NpHR-expressing experimental mouse (*D*) in a three-chamber food preference test.

(*E*) Quantification of the time spent by EYFP and NpHR mice in each chamber. *P* = 0.096; two-way ANOVA followed by Bonferroni *post hoc* analysis.

(*F*) The food preference index of EYFP and NpHR mice. *P* = 0.087; unpaired t test.

(*G* and *H*) The same as (*E* and *F*) but for the time spent in each zone. **P* < 0.05. Error bars indicate mean ± SEM (EYFP, *n* = 10; NpHR, *n* = 10).

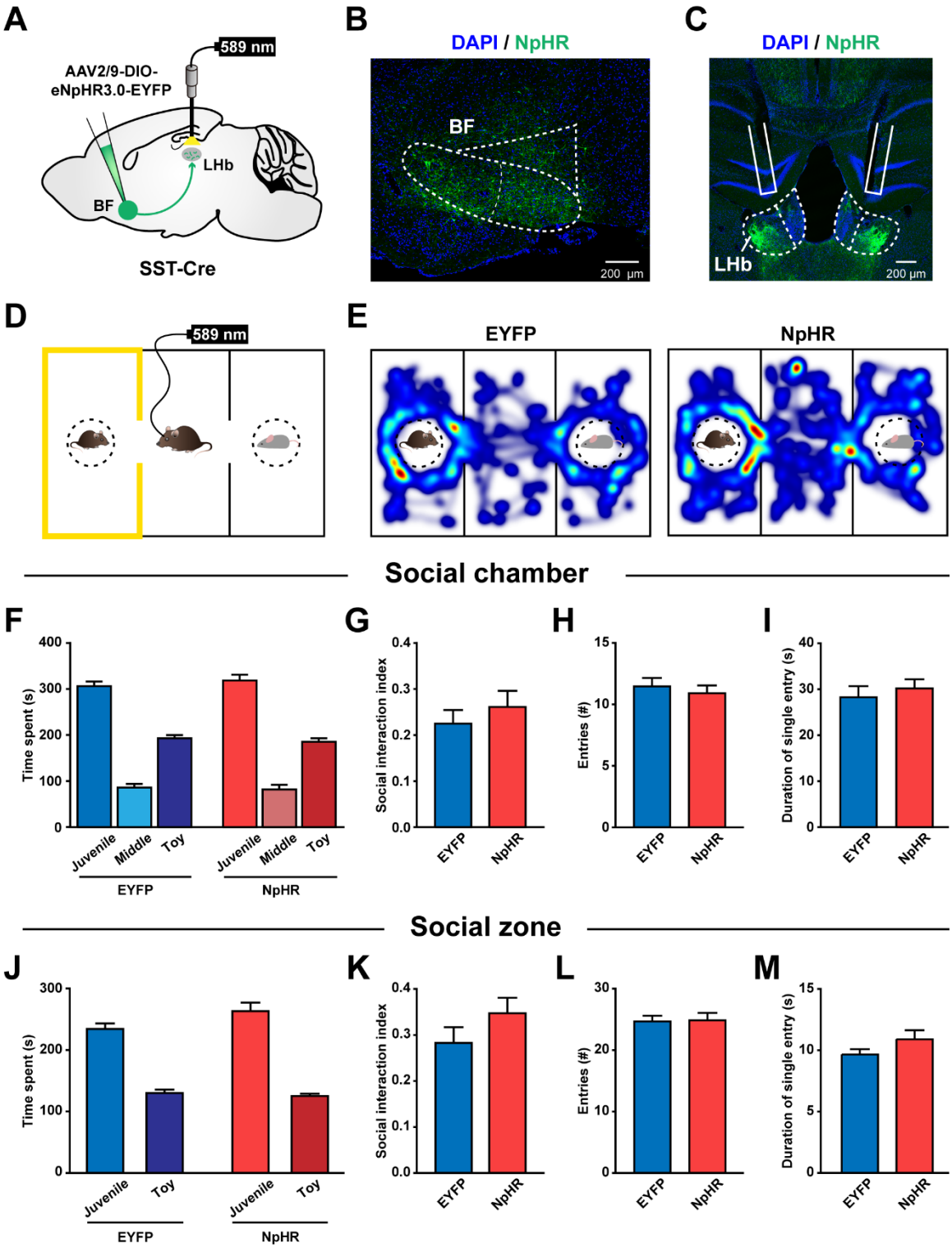

Fig. S7. Optogenetic inhibition of BF SST→LHb projections has no effect on social interaction.

(*A*) Schematic illustration of eNpHR3.0-EYFP virus injection in the BF and optical fiber implantation in the LHb.
(*B* and *C*) Representative images showing NpHR expression in the BF (*B*), and NpHR-expressing axon terminals in the LHb (*C*).
(*D*) Schematic illustration of an experimental mouse subjected to a three-chamber social interaction test, where the social chamber was paired with constant yellow light stimulation (589 nm, 5-8 mW).
(*E*) Representative heatmaps showing the locations of an EYFP-expressing control mouse (Left) and an NpHR-expressing experimental mouse (Right) in a three-chamber social interaction test.
(*F*-*I*) Quantification of social behavioral performance in a three-chamber social interaction test. Note that EYFP mice and NpHR mice exhibited similar time spent in each chamber (*F*), social interaction index (*G*), the number of entries to social chamber (*H*) and mean duration of individual social chamber investigations (*I*).
(*J*-*M*) The same as (*F*-*I*) but for the time spent in each zone.
Error bars indicate mean ± SEM (EYFP, n = 11; NpHR, n = 10).

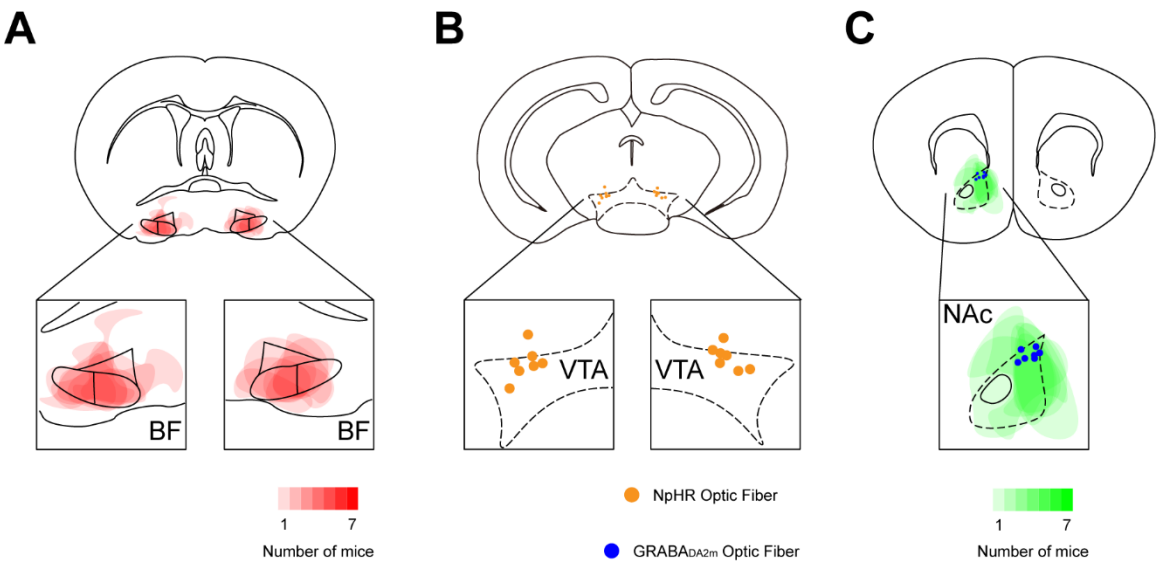

Fig. S8. Viral targeting and fiber placement for $GRAB_{DA2m}$ fluorescence recording and optogenetic suppression of the BF SST→VTA pathway.

(*A*) Overlay of eNpHR3.0-mCherry expression in the BF of 7 SST-Cre mice. Red, viral targeting.

(B) Placement of optical fibers in the VTA. Yellow dots: tips of all optical fibers.

(*C*) Viral targeting and fiber placement for $GRAB_{DA2m}$ fluorescence recording in the NAc. Blue dots: tips of all optical fibers. Green, viral targeting.

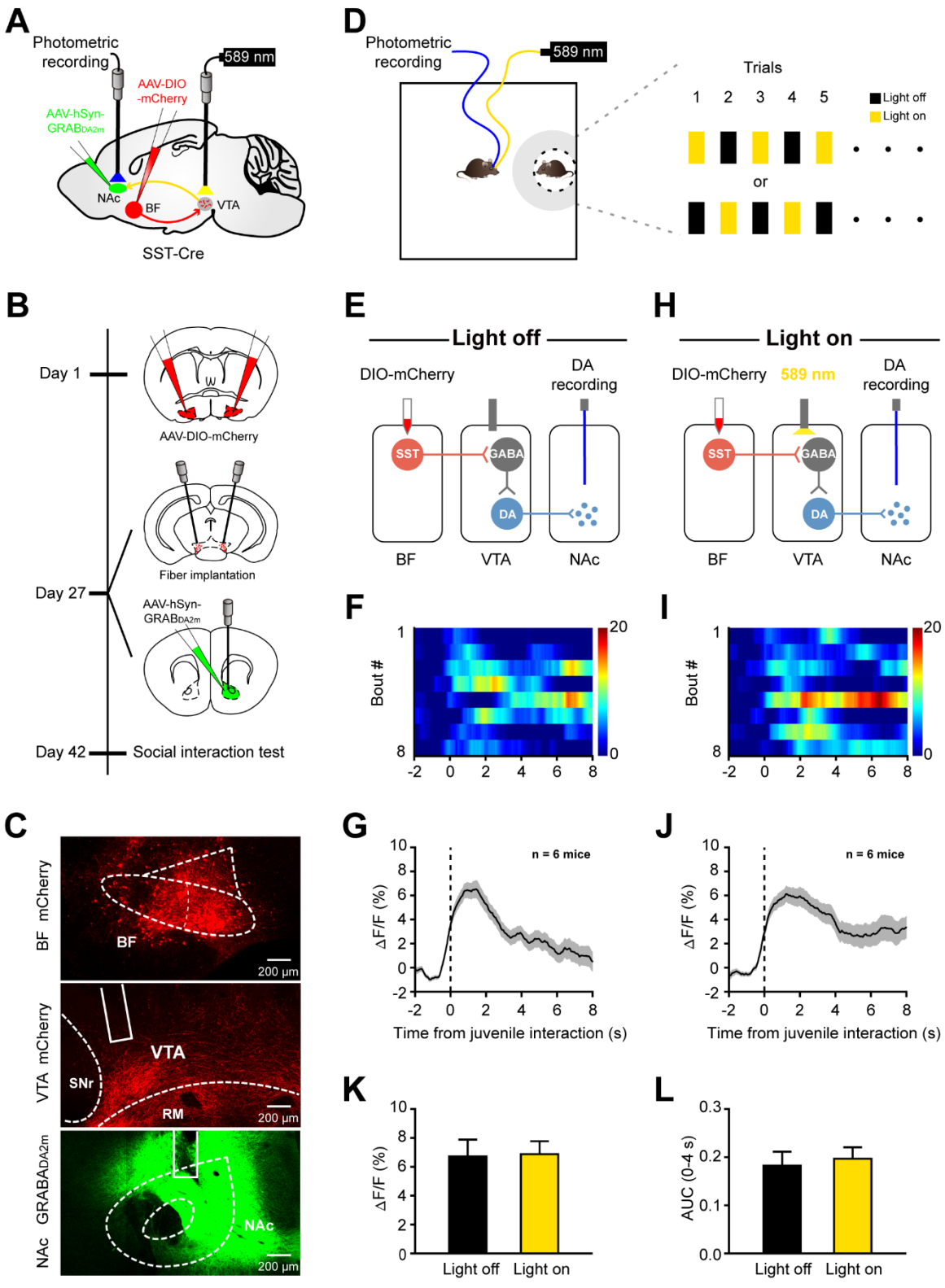

Fig. S9. Yellow light stimulation *per se* does not affect DA release in the NAc during social interaction.

(*A*) Schematic illustration of viral injection, fiber implantation and photometric recording.
(*B*) Time course of the experimental design.
(*C*) Representative images showing mCherry expression in the BF (Top), mCherry-expressing axon terminals in the VTA (Middle), and $GRAB_{DA2m}$ expression in the NAc (Bottom), respectively.
(*D*) Schematic illustration of photometric recording. Mouse entries into the social zone (gray region: 8 cm vicinity) triggered yellow light on half trials at an alternative fashion.
(*E*) Schematic diagram showing photometric recording of NAc DA efflux in Light off trials.
(*F*) Heatmap showing $GRAB_{DA2m}$ fluorescence signals aligned to the onset of individual social interaction in Light off trials. Each row represents one bout. The color scale at the right indicates ΔF/F.
(*G*) Mean $GRAB_{DA2m}$ signal transient during social interaction in Light off trials for the entire test group (n = 6 mice). The thick line indicates mean and the shaded area indicates SEM.
(*H*-*J*) The same as (*E*-*G*) but for Light on trials.
(*K* and *L*) Statistic comparison of $GRAB_{DA2m}$ fluorescence signals during social interaction between Light on and Light off trials. Note that there was no difference in either peak amplitude (*K*) or the AUC (*L*) of $GRAB_{DA2m}$ fluorescence signals between Light off and Light on trials. Error bars indicate mean ± SEM.

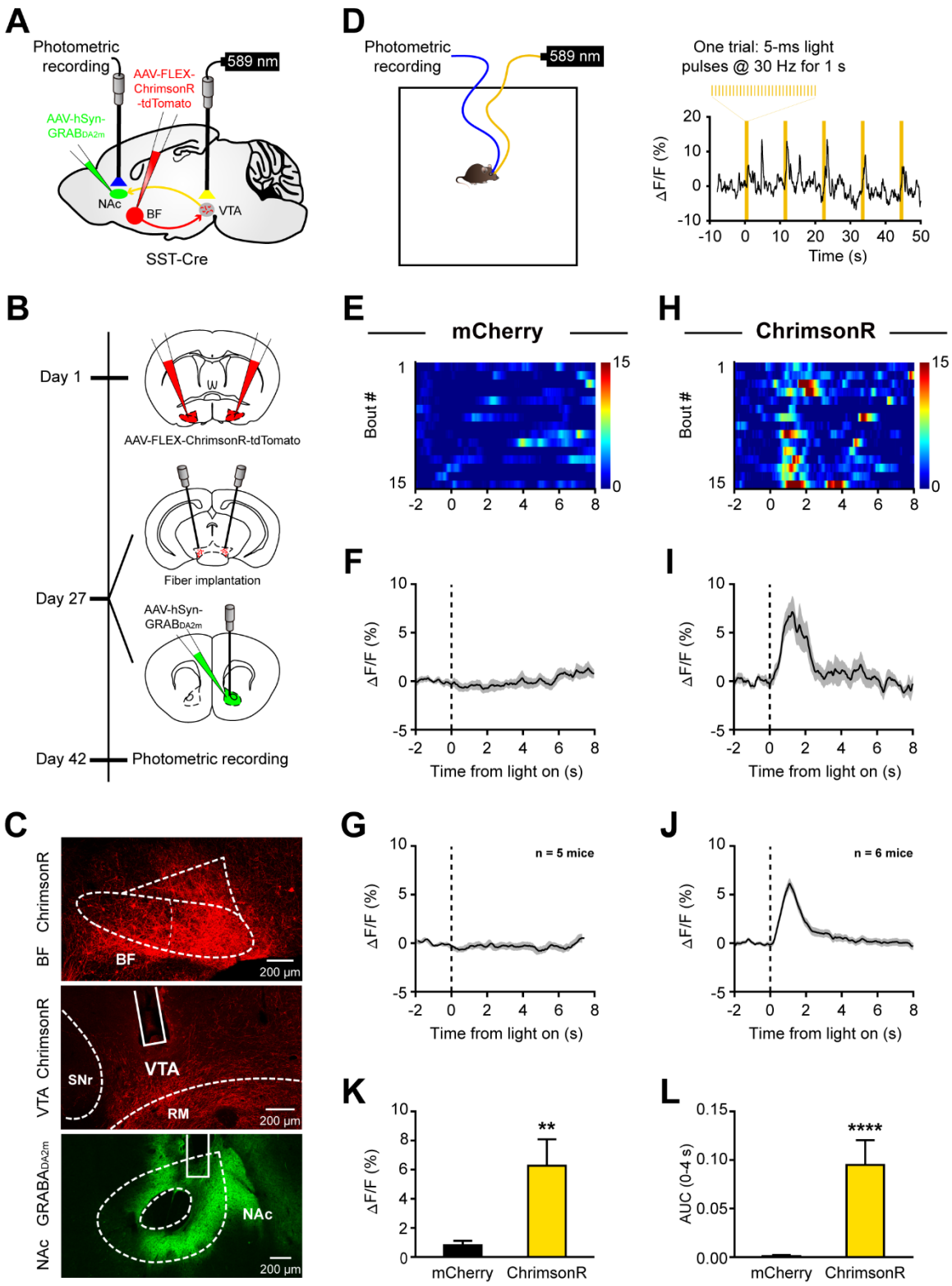

Fig. S10. Fluorescence signals of $GRAB_{DA2m}$ in NAc evoked by optogenetic stimulation of BF SST→VTA projections.

(*A*) Schematic illustration of viral injection, fiber implantation and photometric recording.
(*B*) Time course of the experimental design.
(*C*) Representative images showing ChrimsonR-mCherry expression in the BF (Top), ChrimsonR-expressing axon terminals in the VTA (Middle), and $GRAB_{DA2m}$ expression in the NAc (Bottom), respectively.
(*D*) Left: Schematic illustration of photometric recording in an open field arena. Right: Snapshot of 5 trials showing increases in fluorescence signals evoked by yellow light pulses. Yellow bars indicate 1 s of 30-Hz light stimulus.
(*E*) Representative heatmap showing $GRAB_{DA2m}$ fluorescence signals aligned to the onset of yellow light stimulation in a mouse expressing mCherry in the BF. Each row represents one bout. The color scale at the right indicates ΔF/F.
(*F*) The peri-event plot of the average Ca^{2+} transients of a mCherry mouse showing in (*E*). The thick line indicates mean and the shaded area indicates SEM.
(G) Mean $GRAB_{DA2m}$ signal transient by yellow light stimulation for the entire test group of mCherry mice (n = 5). The thick line indicates mean and the shaded area indicates SEM.
(*H*-*J*) The same as (*E*-*G*) but for ChrimsonR mice (n = 6).
(*K* and *L*) Statistic comparison of $GRAB_{DA2m}$ fluorescence signals in response to yellow light stimulation between mCherry and ChrimsonR mice. Note that activation of BF SST→VTA projections significantly enhanced both the peak amplitude (*K*) and the AUC (*L*) of $GRAB_{DA2m}$ fluorescence signals in ChrimsonR mice compared to those in mCherry mice. Error bars indicate mean ± SEM. $^{**}P < 0.01$; $^{****}P < 0.0001$; unpaired t test.

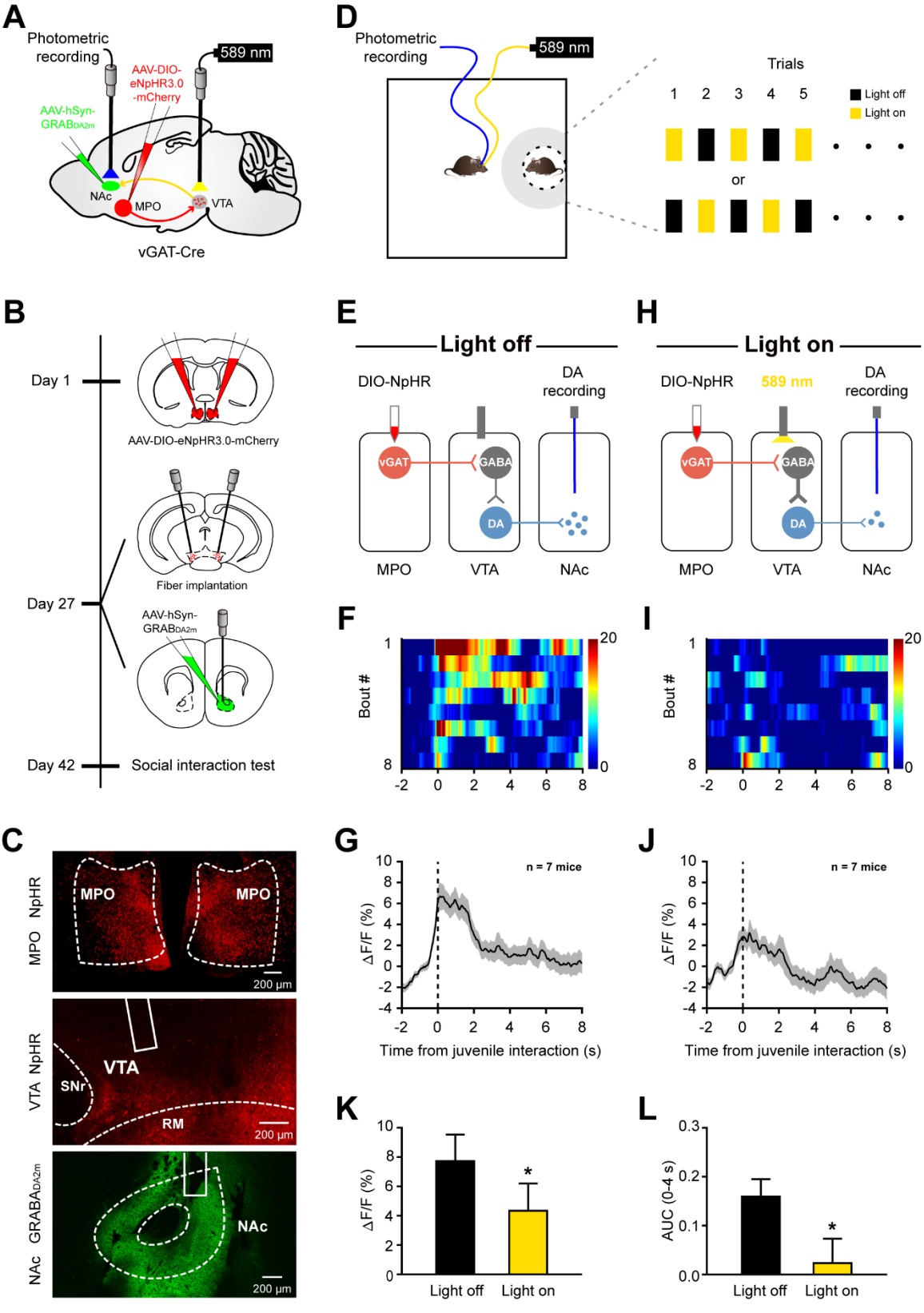
A
Photometric recording
589 nm
AAV-DIO-eNpHR3.0 -mCherry
AAV-hSyn-GRABDA2m
NAc
MPO
VTA
vGAT-Cre
D
Photometric recording
589 nm
Trials
1 2 3 4 5
Light off
Light on
or
B
Day 1
AAV-DIO-eNpHR3.0-mCherry
Fiber implantation
Day 27
AAV-hSyn-GRABDA2m
Day 42
Social interaction test
E
Light off
DIO-NpHR
DA recording
vGAT
GABA
DA
MPO
VTA
NAc
H
Light on
DIO-NpHR
589 nm
DA recording
F
Bout #
I
C
MPO NpHR
VTA NpHR
NAc GRABDA2m
MPO
VTA
SNr
RM
NAc
200 μm
G
n = 7 mice
ΔF/F (%)
Time from juvenile interaction (s)
J
K
Light off
Light on
L
AUC (0-4 s)

Fig. S11. Inhibition of MPO GABA→VTA projections reduces DA release in the NAc during social interaction.

(*A*) Schematic illustration of viral injection, fiber implantation and photometric recording.

(*B*) Time course of the experimental design.

(*C*) Representative images showing NpHR-mCherry expression in the MPO (Top), NpHR-expressing axon terminals in the VTA (Middle), and $GRAB_{DA2m}$ expression in the NAc (Bottom), respectively.

(*D*) Schematic illustration of photometric recording. Mouse entries into the social zone (gray region: 8 cm vicinity) triggered yellow light to inhibit MPO GABA→VTA projections on half trials at an alternative fashion.

(*E*) Schematic diagram showing photometric recording of NAc DA efflux in Light off trials.

(*F*) Heatmap showing $GRAB_{DA2m}$ fluorescence signals aligned to the onset of individual social interaction in Light off trials. Each row represents one bout. The color scale at the right indicates ΔF/F.

(*G*) Mean $GRAB_{DA2m}$ signal transient during social interaction in Light off trials for the entire test group (n = 7 mice). The thick line indicates mean and the shaded area indicates SEM.

(*H*-*J*) The same as (*E*-*G*) but for Light on trials.

(*K* and *L*) Statistic comparison of $GRAB_{DA2m}$ fluorescence signals during social interaction between Light on and Light off trials. Note that inhibition of MPO GABA→VTA projections reduced both the peak amplitude (*K*) and the AUC (*L*) of $GRAB_{DA2m}$ fluorescence signals. Error bars indicate mean ± SEM. *P < 0.05; paired t test.

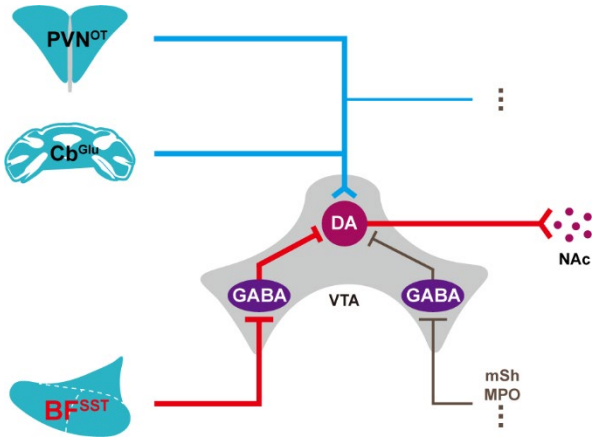

Fig. S12. The integration of multiple social promoting pathways in the VTA. Schematic diagram summarizing multiple social promoting pathways in the VTA. Notably, there are at least two major modes of activity modulation in VTA DA neurons, that is, excitation and disinhibition. Convergent excitatory inputs together with disinhibitory inputs synergistically tune the DA neuron activity and hence control prosocial behavior. Cb, cerebellum; Glu, glutamate; OT, oxytocin; PVN, the paraventricular hypothalamus nucleus; MPO, medial preoptic area; mSh, medial shell of the NAc.